



Improving Biocatalytic Synthesis of Furfuryl Alcohol by Effective Conversion of *D*-Xylose into Furfural with Tin-Loaded Sulfonated Carbon Nanotube in Cyclopentylmethyl Ether-Water Media

Qi Li¹ · Yun Hu¹ · Yong-You Tao¹ · Peng-Qi Zhang¹ · Cui-Luan Ma¹ · Yu-Jie Zhou¹ · Yu-Cai He^{1,2,3}

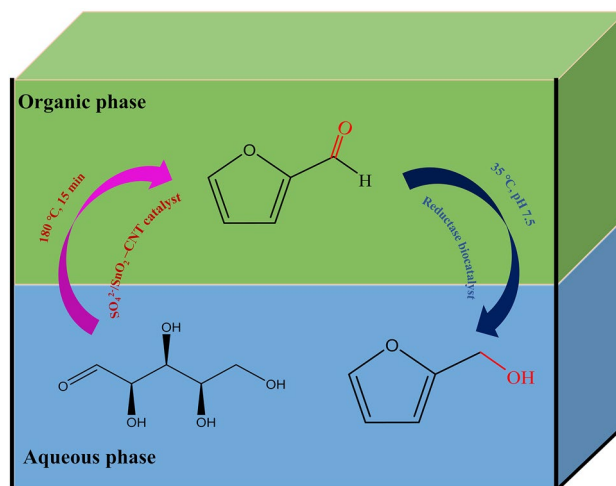
Received: 27 December 2020 / Accepted: 12 February 2021

© The Author(s), under exclusive licence to Springer Science+Business Media, LLC part of Springer Nature 2021

Abstract

Carbon nanotube (CNT) was utilized as as the precursor to synthesize solid acid (tin-loaded sulfonated carbon nanotube, $\text{SO}_4^{2-}/\text{SnO}_2\text{-CNT}$) for catalyzing *D*-xylose into furfural. Fourier transform infrared spectroscopy, Roman spectroscopy, X-ray diffraction analysis, and scanning electron microscope techniques were used for characterizing $\text{SO}_4^{2-}/\text{SnO}_2\text{-CNT}$. Different loading of *D*-xylose (20–100 g/L) were converted into furfural (81.6–299.1 mM) at 41.9–61.2% yield by $\text{SO}_4^{2-}/\text{SnO}_2\text{-CNT}$ (3.5 wt%) within 15 min at 180 °C in cyclopentylmethyl ether-water (1:2, v:v) biphasic media. Subsequently, whole-cells of recombinant *Escherichia coli* CG-19 cells expressing reductase catalyzed *D*-xylose-derived furfural at 35 °C and pH 7.5. Within 3 h, the prepared *D*-xylose (81.6–299.1 mM) could be converted into furfuryl alcohol at 32.7–61.2% yield (based on the *D*-xylose loading). Sequential conversion of *D*-xylose with $\text{SO}_4^{2-}/\text{SnO}_2\text{-CNT}$ and reductase catalysts was established for the effective production of furfuryl alcohol.

Graphic Abstract



Keywords *D*-Xylose · Furfural · Furfuryl alcohol · Reductase · Sulfonated $\text{SO}_4^{2-}/\text{SnO}_2\text{-CNT}$

Qi Li and Yun Hu have contributed equally to this work.

✉ Cui-Luan Ma
macuiluan@163.com

✉ Yu-Cai He
heyucai2001@163.com

Extended author information available on the last page of the article

1 Introduction

Lignocellulosic biomass is widely used as renewable substitute for conventional fossil resources for sustainable production of biobased chemicals, functional materials, bio-fuel molecules, and etc. Furfural (FF), a versatile platform

molecule, has been highlighted as one of the top ten most rewarding bio-based building-blocks by the US Department of Energy (DOE). It is mainly derived from the C5-sugars in lignocellulosic biomass, has been studied and utilized extensively due to its industrial availability and importance [1, 2]. FF molecule contains both C=O group in branched-chain and C=C bonds in furan ring, which is known as a versatile precursor for industrially manufacturing biofuels, fine chemicals, food flavors, resins, solvents, fragrances, fungicides, lubricating oils, nematicides, and plastics [3–7]. Industrially, homogeneous inorganic and organic acids are chosen for transforming pentose (mainly *D*-xylose) to FF [7, 8]. To this date, numerous heterogeneous solid acids (carbon, sulfonated attapulgite, sulfonated montmorillonite, functional resin, modified TiO₂-ZrO₂, H-ZSM-5, modified zeolite, etc.) [9–13] exhibit superior performances and good catalytic characteristics for manufacturing FF via *D*-xylose-dehydration reactions.

Among FF-upgrading chemicals, furfuryl alcohol (FFA) is the hydrogenation product of FF through the reduction of the C=O bond in FF molecule. It is widely used for the synthesis of biofuels, cements, lubricants, additives, plastics, adhesives, resins, coatings, dyes and solvents. FFA can be manufactured through hydrogenation of FF, either in liquid or vapor phase [14–17]. However, the drawback is the low selectivity to FFA. Copper chromite with moderate catalytic activity and high toxicity has been used in the selective hydrogenation of FF to FFA at high-temperature (130–200 °C) and high H₂ pressure [17, 18]. An electro-synthetic approach yielded nearly 90% of FFA from FF in acetonitrile media containing 0.50 M H₂SO₄ [19]. Cu/SBA-15-SO₃H catalyzed *D*-xylose to FFA with 63% yield for 6 h at 140 °C under the high-pressure (4.0 MPa) in *n*-butanol-water biphasic media [20]. Compared with conventional chemical catalysis, the use of microorganisms for whole-cell catalysis of FF to FFA is considered as a sustainable and green alternative. *B. coagulans*, *E. coli*, *M. deltae*, and *S. cerevisiae* could convert FF to FFA under mild conditions [21–24].

It is known that *D*-xylose can be effectively converted into FF by heterogeneous catalyst in cyclopentylmethyl ether-water biphasic media [7]. In our study, carbon nanotube (CNT) as heterogeneous solid acid support was used to synthesize tin-loaded sulfonated SO₄²⁻/SnO₂-CNT catalyst for catalyzing *D*-xylose into FF in cyclopentylmethyl ether-water biphasic media. Fourier transform infrared spectrum, X-ray diffraction, scanning electron microscope, and nitrogen adsorption/desorption isotherms were characterized the SO₄²⁻/SnO₂-CNT. Moreover, biocatalytic upgrading of FF into FFA by recombinant reductase biocatalyst was conducted under the environmentally-friendly conditions. Finally, *D*-xylose was tandemly catalyzed into FFA were established by sequential catalysis with sulfonated

SO₄²⁻/SnO₂-CNT catalyst and reductase biocatalyst in cyclopentylmethyl ether-water biphasic media.

2 Materials and Methods

2.1 Materials and Chemicals

Carbon nanotube (CNT) was purchased from Suzhou Tanfeng Graphene Technology Co., Ltd. (Jiangsu, P.R. China). Ammonia (NH₃•H₂O), cyclopentylmethyl ether (CPME), *D*-xylose, ethanol, and furfural (FF) and chemicals were obtained from Lingfeng Chemical Reagent Co., Ltd. (Shanghai, P.R. China).

2.2 Synthesis of Sulfonated SO₄²⁻/SnO₂-CNT

2.8 g SnCl₄, 8.4 g CNT and 180.0 g ethanol were blended in 500 mL glass beaker by the agitation with magnetic stirrer at room temperature. The formed homogeneous turbid liquid was regulated to pH 6.0 by addition of NH₃•H₂O (25.0 wt%). This colloidal solution was dried in an oven at 70 °C over 10 h and kept at 90 °C for 12 h. Subsequently, the oven-dried solid was immersed in 120.0 mL 1.0 M H₂SO₄ for 3 h, then filtrated and oven-dried at 110 °C for 3.5 h and baked in muffle furnace at 500 °C for another 3.5 h. The resultant SO₄²⁻/SnO₂-CNT was used as catalyst for catalyzing *D*-xylose into FF.

2.3 Cultivation of Recombinant *E. coli* CG-19 Expressing Reductase

Recombinant *E. coli* CG-19 expressing reductase [2] was used to catalyze *D*-xylose-derived FF into FFA. The cultures were inoculated at an OD₆₀₀ of 0.10 at 37 °C. Isopropyl-beta-*D*-thiogalactoside (IPTG) was added to achieve a final concentration of 0.50 mM in order to induce gene expression when the OD₆₀₀ reached 0.60. After induction, the broth was further cultured at 25 °C. After 12 h, cells were isolated by centrifugation (10,000×g) for 5 min at 4 °C.

2.4 Conversion of *D*-Xylose into FF and FFA

Dehydration of *D*-xylose to FF was carried out in this 100-mL autoclave, which contained 40.0 mL mixture of *D*-xylose (20–100 g/L) and SO₄²⁻/SnO₂-CNT (0.5–5.0 wt% dosage) in CPME-water media (0:1–2:1, v/v; pH 1.2). The reaction mixture was quickly heated to the target catalytic temperature (160–180 °C) by a heating jacket and maintained for 5–60 min. The *D*-xylose-derived FF was determined with HPLC. Furthermore, the pH of this resulted FF liquor was regulated to 7.5, and followed by addition of 4.0 g *E. coli*

CG-19 wet cell. The FF-oxidizing reaction was conducted at 35 °C by the agitation of 300 rpm with magnetic stirrer.

2.5 Analytical Methods

CNT and $\text{SO}_4^{2-}/\text{SnO}_2\text{-CNT}$ were analyzed with Fourier transform infrared spectroscopy, Roman spectroscopy, X-Ray diffraction analysis, and scanning electron microscope techniques [10]. Nitrogen adsorption–desorption Isotherms of CNT and $\text{SO}_4^{2-}/\text{SnO}_2\text{-CNT}$ were determined by Brunauer–Emmett–Teller (BET) measurement using a Micromeritics ASAP 2020 surface area analyzer and porosimetry system (Micromeritics Co.). Monomeric sugars were measured with HPLC (Model 2695; Waters Co., Milford, MA, USA) with an Bio-Rad Aminex HPX-87P column (Hercules, CA, USA) [25, 26]. FF and FFA was quantified by HPLC with Waters NovaPak C18 column [6].

3 Results and Discussion

3.1 Characterization of $\text{SO}_4^{2-}/\text{SnO}_2\text{-CNT}$

Carbon nanotubes (CNTs) have been used as versatile supports for catalysts, adsorbents and functional materials, mainly due to their ultra-small size, large specific surface area, high thermostability and unique structure [27–31]. In this case, CNT was used as heterogeneous solid acid catalyst support to prepare sulfonated $\text{SO}_4^{2-}/\text{SnO}_2\text{-CNT}$ for catalyzing *D*-xylose to FF. To observe the unique characteristics of tin-loaded sulfonated CNT catalyst, several analytical techniques were employed on $\text{SO}_4^{2-}/\text{SnO}_2\text{-CNT}$. The analytical results were described below.

The $\text{SO}_4^{2-}/\text{SnO}_2\text{-CNT}$ surface and pore changes were analyzed using nitrogen adsorption/desorption isotherms. As depicted as in Table 1, shows a BET of 225.3 m^2/g , a pore volume of 0.84 m^3/g and a pore width of 14.8 nm. By comparison with CNT, $\text{SO}_4^{2-}/\text{SnO}_2\text{-CNT}$ had an enlarged pore volume, bigger pore size and lower specific surface area. In the synthesis of heterogeneous $\text{SO}_4^{2-}/\text{SnO}_2\text{-CNT}$, various performance conditions including solvent treatment, sulfonation reaction and calcination temperature might affect some components and pore structures of CNT. The surface structures of $\text{SO}_4^{2-}/\text{SnO}_2\text{-CNT}$ and CNT were

Table 1 Surface and pore structure difference of CNT and $\text{SO}_4^{2-}/\text{SnO}_2\text{-CNT}$

Sample	BET surface area, $\text{m}^2 \text{g}^{-1}$	Pore volume, $\text{cm}^3 \text{g}^{-1}$	Pore size, nm
CNT	235.7	0.76	12.9
$\text{SO}_4^{2-}/\text{SnO}_2\text{-CNT}$	225.3	0.84	14.8

also analyzed with SEM spectra (Fig. 1), and the surface of CNT in $\text{SO}_4^{2-}/\text{SnO}_2\text{-CNT}$ had clear particle adhesion. The functional groups of $\text{SO}_4^{2-}/\text{SnO}_2\text{-CNT}$ and CNT were determined by FTIR spectra (Fig. 2). The peaks at near 3433 cm^{-1} (–OH stretching vibration on CNT), 1383 cm^{-1} (stretching vibration of C=O) [10] and 1172 cm^{-1} (non-symmetric stretching vibration of C–O–C or the stretching vibration of sulfur-oxygen double bonds of SO_4^{2-}) were detected. As depicted as XRD spectra (Fig. 3), characteristic diffraction peaks near 26° and 44° of CNT appeared before and after $\text{SO}_4^{2-}/\text{SnO}_2\text{-CNT}$ preparation, indicating that the main CNT structure was maintained. Moreover, the characteristic peaks of SnO_2 were appeared at near 26°, 33°, 51°, and 65°, and the diffraction peaks of 26° overlapped with those of CNT to be masked. The Raman spectra indicated that $\text{SO}_4^{2-}/\text{SnO}_2\text{-CNT}$ maintained a high consistency with CNT (Fig. 4). Two prominent peaks at near 1580 and 1380 cm^{-1} , which represents G-band and D-band [28], respectively. D-band represents the sp^3 defect and disorder, and G-band is ascribed to the sp^2 carbon in CNT. In view of above-mentioned results,

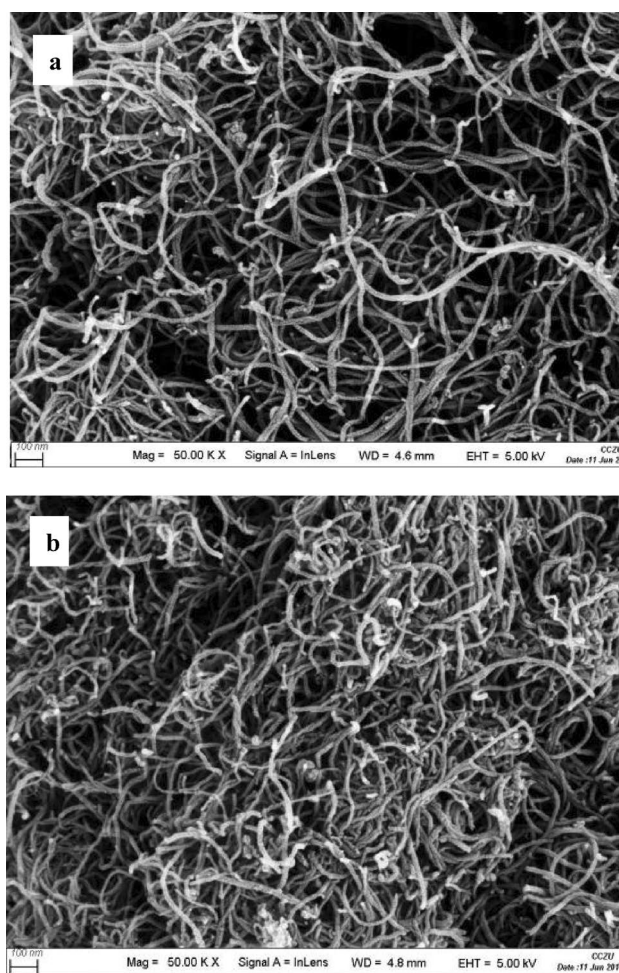


Fig. 1 SEM analysis of CNT (a) and $\text{SO}_4^{2-}/\text{SnO}_2\text{-CNT}$ (b)

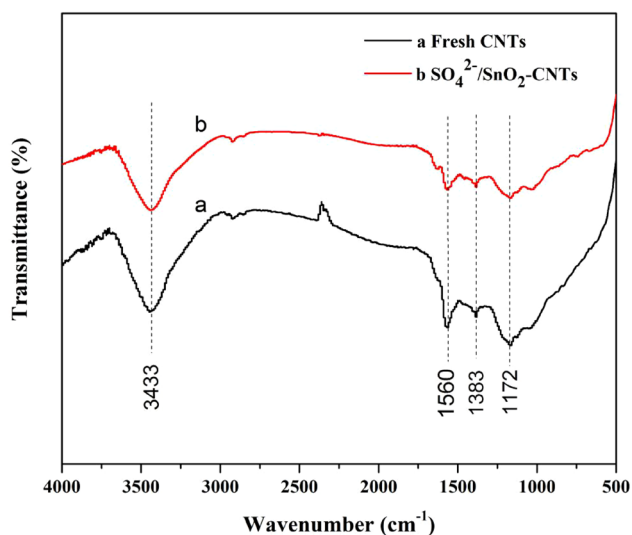


Fig. 2 FT-IR analysis of CNT and $\text{SO}_4^{2-}/\text{SnO}_2\text{-CNT}$

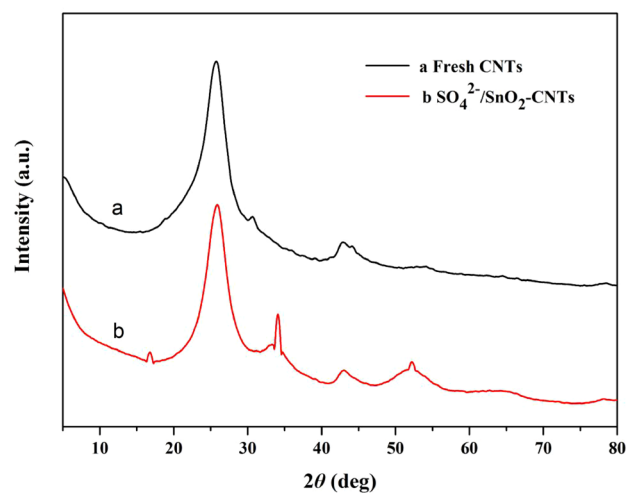


Fig. 3 XRD analysis of CNT and $\text{SO}_4^{2-}/\text{SnO}_2\text{-CNT}$

it was found that the $\text{SO}_4^{2-}/\text{SnO}_2\text{-CNT}$ preparation process had no influence the main structure of CNT.

3.2 Catalysis of *D*-Xylose to FF with $\text{SO}_4^{2-}/\text{SnO}_2\text{-CNT}$

Synthesis of FF in organic solvent–water biphasic media have received much attention, mainly because the newly formed FF in the aqueous phase can be simultaneously extracted into the organic phase [1, 33]. Non water-miscible organic solvent such as cyclopentylmethyl ether (CPME) is known as a promising green co-solvent to extract FF formed in aqueous phase in order to prevent its unwanted degradation or cross polymerization [7, 32, 33]. The volumetric

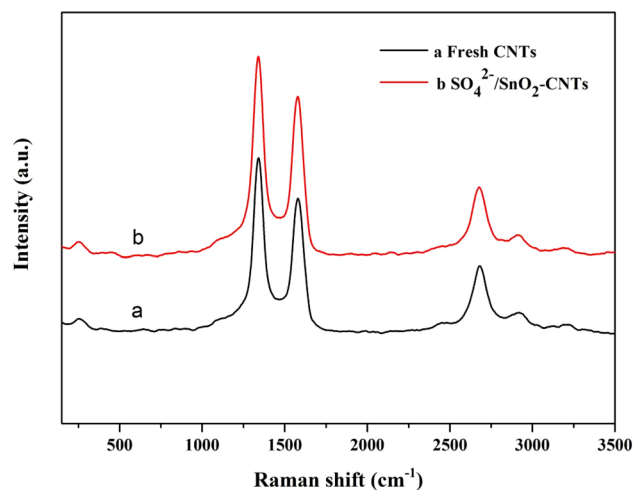


Fig. 4 Raman images of fresh CNT and solid acid $\text{SO}_4^{2-}/\text{SnO}_2\text{-CNT}$

ratio of CPME to H_2O can influence the product FF distribution during the dehydration of substrate *D*-xylose. In 40 mL biphasic media, the CPME phase to water phase ratio was varied for 0:1, 3:1, 2:1, 1:1, and 1:2 (Fig. 5a). Conversions in the CPME–water biphasic media containing different volume ratio of CPME phase to water phase were performed by using 2.5 wt% $\text{SO}_4^{2-}/\text{SnO}_2\text{-CNT}$ catalyst at 180 °C for 15 min to catalyze *D*-xylose into product FF. As indicated in Fig. 5a, when the volume ratio of CPME-to-water was increased from 0:1 to 1:2, the FF yield was raised from 42.1 to 61.2%. By increasing the volumetric ratio from 1:2 to 1:1, FF yield increased slightly. When the ratio was increased from 1:1 to 2:1, FF yield dropped from 62.0 to 53.4%. The appropriate volumetric ratio of CPME-to-water was chosen as 1:2. When the volumetric ratio of water phase increased, the extraction of FF to the CPME phase might be insufficient and the rehydration of FF would be enhanced. While excessive CPME could dilute the dehydration system, reduced the contact opportunity of substrate *D*-xylose to catalyst $\text{SO}_4^{2-}/\text{SnO}_2\text{-CNT}$, and caused the decrease of product FF yields.

During the preparation of FF, catalyst doses, catalytic temperature, catalytic time and substrate loading had significant influence on the FF production [8–12]. In CPME–water (1:2, v:v) media, several reaction parameters including $\text{SO}_4^{2-}/\text{SnO}_2\text{-CNT}$ dosage, catalytic temperature (150–190 °C), catalytic time (10–30 min) and *D*-xylose loading (20–100 g/L) were investigated on the FF production. The effects of catalyst $\text{SO}_4^{2-}/\text{SnO}_2\text{-CNT}$ (2.5–4.5 wt%) on the FF production in CPME–water (1:2, v:v) were evaluated (Fig. 5b). With the increase of $\text{SO}_4^{2-}/\text{SnO}_2\text{-CNT}$ dose from 2.5 to 3.5 wt%, the FF yields increased from 45.0 to 61.2%. When the $\text{SO}_4^{2-}/\text{SnO}_2\text{-CNT}$ dose increased from 3.5

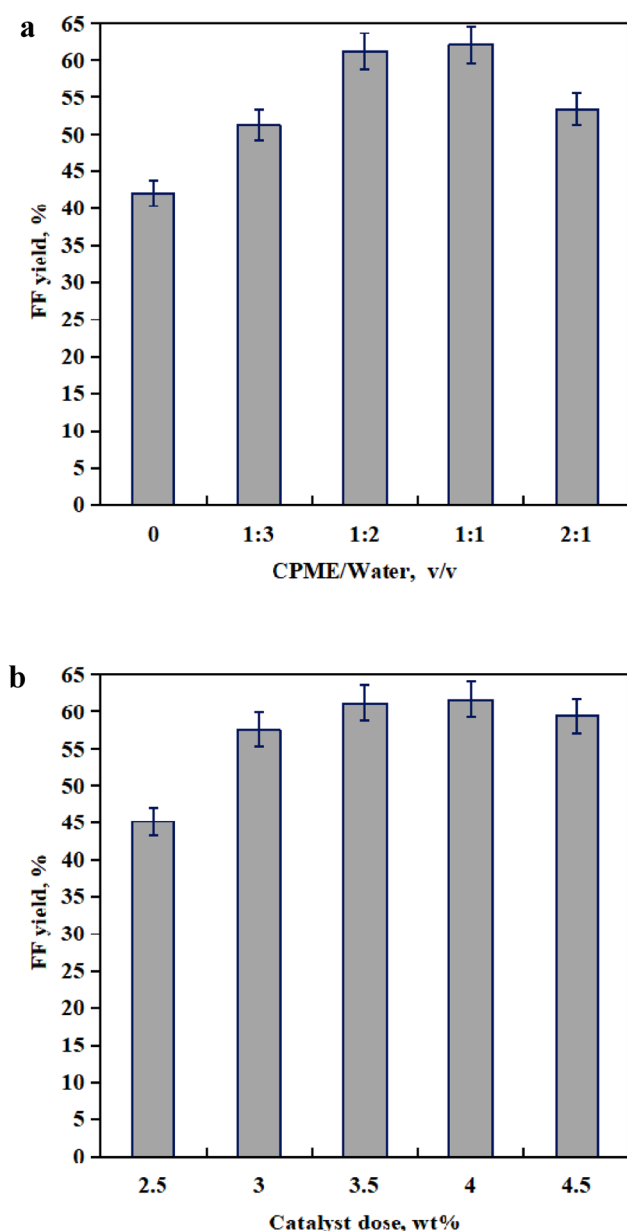


Fig. 5 Effects volumetric ratio of CPME versus water (0:1–2:1) in CPME-water media (a) [*D*-xylose loading 20 g/L, catalyst loading 3.5 wt%, 180 °C, 15 min]; Effects catalyst $\text{SO}_4^{2-}/\text{SnO}_2\text{-CNT}$ loading (2.5–4.5 wt%) in CPME-water (1:2, v:v) media (b) [*D*-xylose loading 20 g/L, 180 °C, 15 min]

to 4.0 wt%, the yields of FF had no significant change. At over 4.0 wt%, FF yield decreased slightly. Thus, the appropriate Sn-PL dose was 3.5 wt%. After commercial *D*-xylose (20.0 g/L) was catalyzed by 3.5 wt% $\text{SO}_4^{2-}/\text{SnO}_2\text{-CNT}$ for 15 min at 150–190 °C, FF yields and selectivities increased clearly from 150 to 180 °C (Fig. 6a). At 180 °C, FF yield and selectivity were obtained at 61.2% and 95.0%, respectively. By increasing the catalytic temperature from 180 to

190 °C, the FF yields had no significant increase. Thus, the optimum catalytic temperature for converting *D*-xylose was 180 °C. After commercial *D*-xylose (20.0 g/L) was catalyzed by 3.5 wt% $\text{SO}_4^{2-}/\text{SnO}_2\text{-CNT}$ for 10–30 min at 180 °C, FF yields and selectivities increased clearly from 10 to 15 min (Fig. 6b). Over 15 min, FF yields and selectivities had no significant change. Thus, the optimum catalytic time for converting *D*-xylose was 15 min. In CPME-water (1:2, v:v) media, high FF yield was obtained at 61.2% when commercial *D*-xylose (18.0 g/L) was catalyzed by 3.5 wt% $\text{SO}_4^{2-}/\text{SnO}_2\text{-CNT}$ for 15 min at 180 °C. Different loadings of *D*-xylose (20–100 g/L) were used for the synthesis FF for 15 min at 180 °C (Fig. 6c). By increasing *D*-xylose loading from 20 to 60 g/L, FF yields decreased from 61.2 to 51.2%. Using 80 and 100 g/L of *D*-xylose as substrates, FF yields were obtained at 46.7% and 44.9%, respectively. It was found that *D*-xylose conversion had no significant change, while FF yield and FF selectivity gradually decreased.

The reuse of catalyst can reduce the economic burden [10]. To evaluate the stability of $\text{SO}_4^{2-}/\text{SnO}_2\text{-CNT}$ catalyst, this heterogeneous and reusable catalyst was recycled and reused for five times to catalyze *D*-xylose (20 g/L) into FF for 15 min at 180 °C. After each catalytic round, $\text{SO}_4^{2-}/\text{SnO}_2\text{-CNT}$ was recovered by filtration, washed with deionized water and ethanol for three times to remove some residues and oven-dried at 100 °C. It was observed that the FF yields gradually dropped after each recycle (Fig. 7). From 1st to 6th run, FF yield dropped from 61.2 to 48.3%, indicating a comparable stable recycle capacity. Heterogeneous solid acid catalysts have received an increase attention because of their excellent performance stability and easily recycling properties for manufacturing high-value-added biobased chemicals [34].

3.3 Biotransformation of *D*-Xylose-Derived FF into FFA

Biocatalysis is nowadays an established technology for the production of high-value-added chemicals with high catalytic activity and selectivity under mild conditions [35–37]. FF is a major microbial inhibitor [6, 38]. Using commercial FF as substrate, FF (≤ 100 mM) could be completely consumed by *E. coli* CG-19 cells within 3 h (Fig. 8). At over 100 mM, FFA yields decreased clearly.

The cascade catalysis by chemoenzymatic reaction without isolation of any intermediates has attracted a considerable interest due to short performance time [2]. In this study, tandem catalysis of *D*-xylose (20–100 g/L) to FFA was conducted via sequential conversion with $\text{SO}_4^{2-}/\text{SnO}_2\text{-CNT}$ catalyst and CG-19 reductase biocatalyst in a sealed autoclave. Firstly, different loading of *D*-xylose (20–100 g/L) were converted into FF in 40 mL CPME-water (1:2, v:v) for 15 min

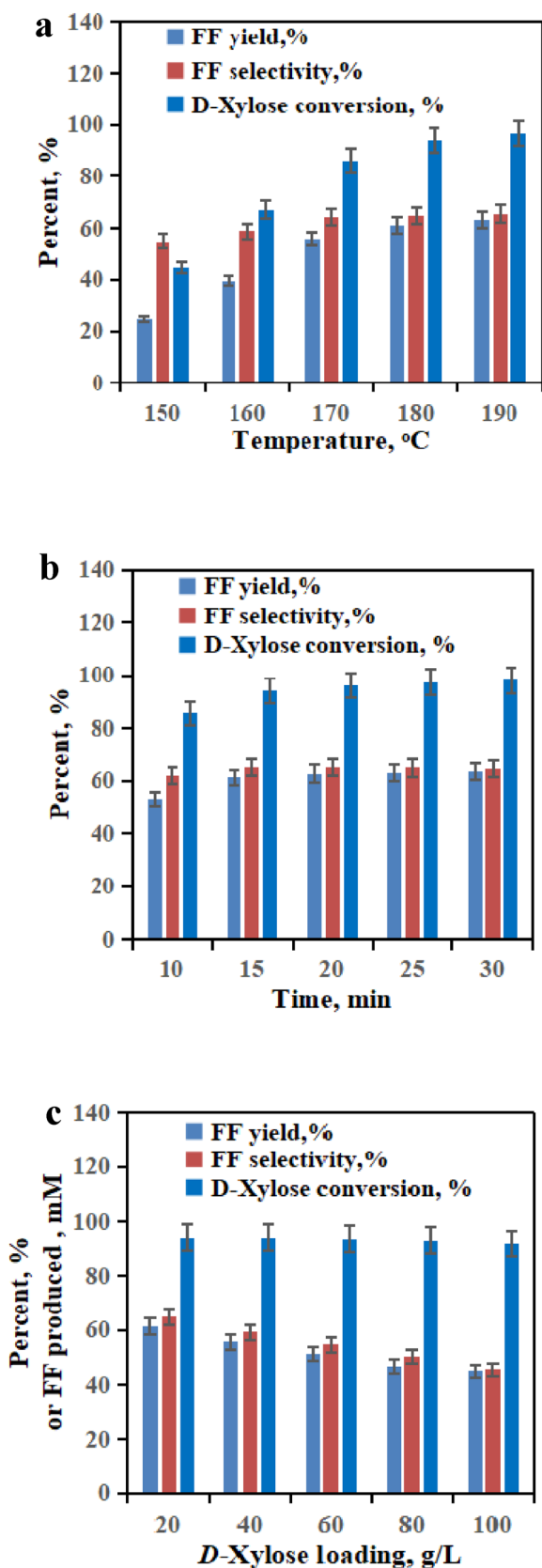


Fig. 6 Effects of reaction temperature (150–190 °C) (a), reaction time (10–30 min) (b), and *D*-xylose loading (20–100 g/L) (c) on the FF yield and selectivity in CPME-water (1:2, v:v) media

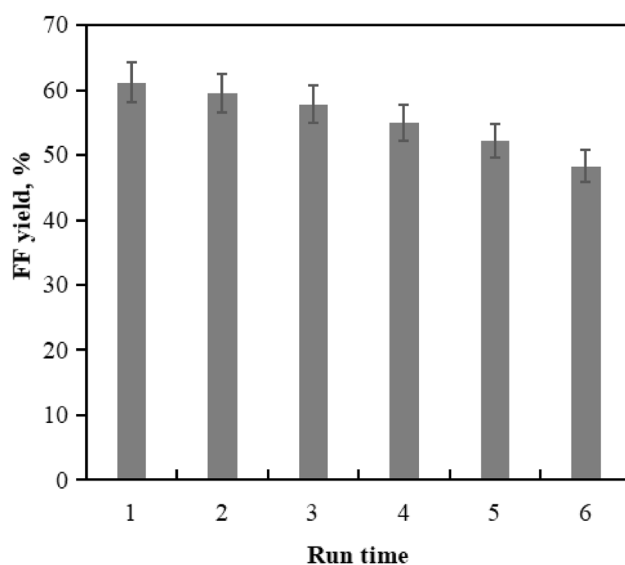


Fig. 7 Recycle and reuse of $\text{SO}_4^{2-}/\text{SnO}_2\text{-CNT}$ [in CPME-water (1:2, v:v) media [*D*-xylose loading 20 g/L, initial $\text{SO}_4^{2-}/\text{SnO}_2\text{-CNT}$ loading 3.5 wt%, 180 °C, 15 min]

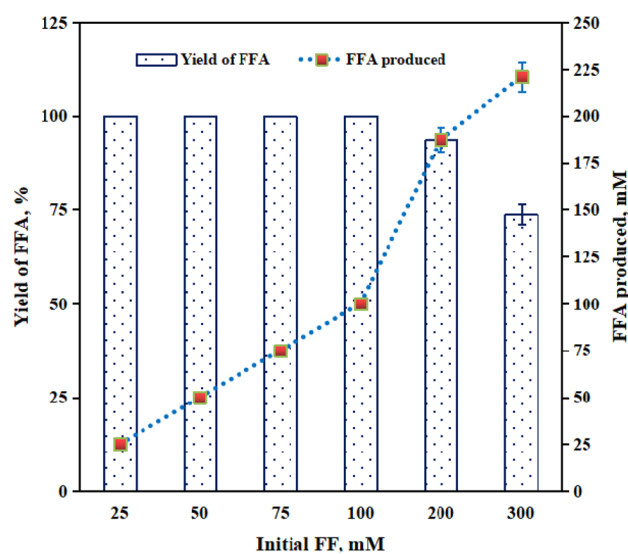


Fig. 8 Effects of initial FF doses (25–300 mM; commercial FF) on the production of FFA by whole-cells

at 180 °C. Subsequently, the prepared *D*-xylose-derived FF liquors (81.6 mM, 148.5 mM, 204.8 mM, 248.9 mM, and 299.1 mM) were regulated to pH 7.5 with 3.0 M sodium hydroxide. Dilute FF liquors (42.0 mL) were biologically converted into FFA at 35 °C by adding 4.0 g whole-cells of recombinant *E. coli* CG-19 expressing reductase. Without isolation of $\text{SO}_4^{2-}/\text{SnO}_2\text{-CNT}$, FFA yields (based on the *D*-xylose loading) decreased from 61.2 to 38.3% by increasing the *D*-xylose loading from 20 to 80 g/L within 3 h in 42.0 mL media (Fig. 9). At 100 g/L of *D*-xylose, the overall

yield of FFA was obtained at 32.7% (218.0 mM FFA). Compared with the hydrogenation of FF to FFA in liquid or vapor phase [15–19], synthesis of FFA could be efficiently conducted via chemoenzymatic approach by sequential catalysis of *D*-xylose with $\text{SO}_4^{2-}/\text{SnO}_2\text{-CNT}$ and reductase biocatalysis under the relatively mild conditions (Fig. 10).

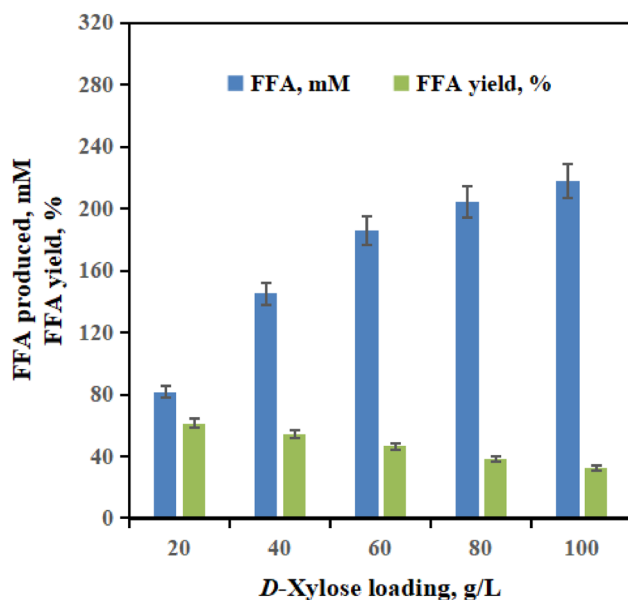
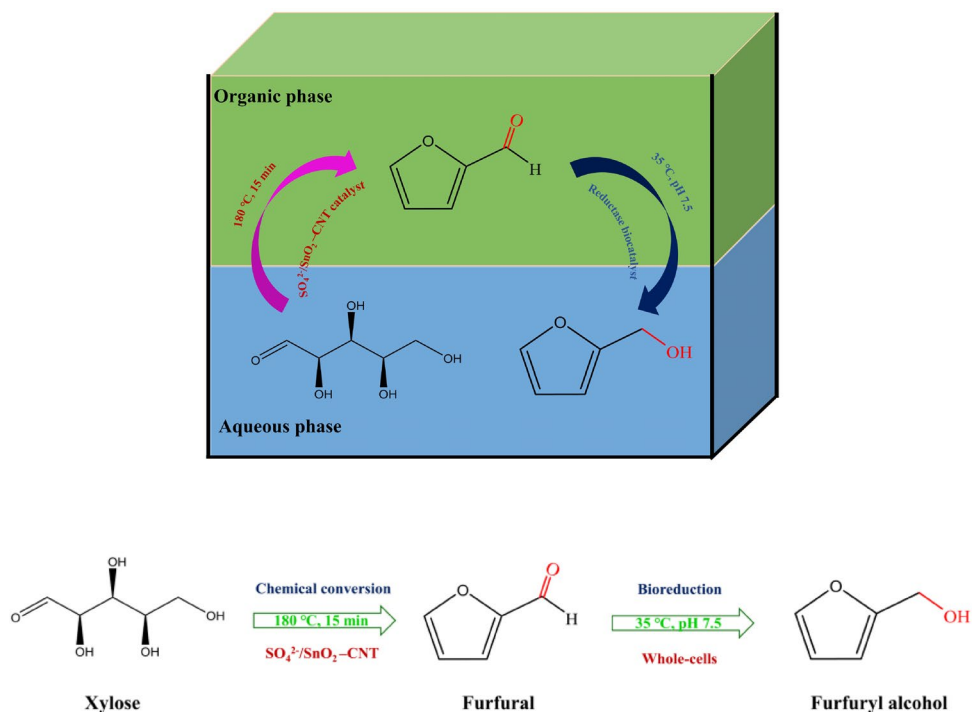


Fig. 9 Effects of initial *D*-xylose doses (20–100 g/L) on the production of FFA via chemoenzymatic conversion

Fig. 10 Tandem conversion of *D*-xylose into FFA via chemoenzymatic conversion



By using the available biomass or biomass-derived *D*-xylose, various biobased chemicals have been manufactured via chemo- and/or enzymatic routes [39–42]. One of important biobased chemicals is FF, largely produced from the dehydration of *D*-xylose, the main monomer of hemicellulose-rich biomass. FFA is a versatile furan-based chemical, which can be obtained through catalytic upgrading of FF via chemical or biocatalytic approach [43–47]. It has attracted considerable interest to manufacture high-value-added FFA by biocatalyst due to its reductase activity and selectivity under environmentally-friendly conditions [2, 43]. Thus, this study provided a chemoenzymatic strategy for tandemly transforming biomass-derived *D*-xylose into FFA by $\text{SO}_4^{2-}/\text{SnO}_2\text{-CNT}$ catalyst and CG-19 reductase biocatalyst in CPME-water (1:2, v:v) media.

4 Conclusion

Using *D*-xylose (20–100 g/L) as feedstocks, FF (81.6–299.1 mM) could be obtained at 44.9–61.2% by 2.5 wt% $\text{SO}_4^{2-}/\text{SnO}_2\text{-CNT}$ for 15 min at 180 °C in CPME-water (1:2, v:v) media. Subsequently, *D*-xylose-derived FF was effectively biotransformed to FFA by CG-19 cells within 3 h. A sustainable and effective route for catalyzing biomass-derived *D*-xylose into FFA was successfully established via sequential chemical catalysis and biocatalysis.

Acknowledgements All authors acknowledge support from NSFC (National Natural Science Foundation of China) (21978072) and the Open Project of Jiangsu Key Laboratory for Biomass-based Energy and Enzyme Technology (BEETKB1902).

References

- Li H, Chen X, Ren J et al (2015) *Biotechnol Biofuels* 8:127
- Li YY, Li Q, Zhang PQ et al (2021) *Bioresour Technol* 320:124267
- Le Guenic S, Gergela D, Ceballos C et al (2016) *Molecules* 21:1102
- Dedes G, Karnaouri A, Topakas E (2020) *Catalysts* 10:74
- Hashim LH, Halilu A, Sudarsanam P et al (2020) *Fuel* 275:117953
- Wang ZW, Gong CJ, He YC (2020) *Bioresour Technol* 303:122930
- Wen M, Zhang XP, Zong MH et al (2020) *J Energ Chem* 41:20–26
- Yang T, Li WZ, Su MX et al (2020) *New J Chem* 44:7968–7975
- Delbecq F, Takahashi Y, Kondo T (2018) *Catal Commun* 110:74–78
- Gong L, Xu ZY, Dong JJ et al (2019) *Bioresour Technol* 293:122065
- Wang YT, Delbecq F, Kwapinski W et al (2017) *Mol Catal* 438:167–172
- Ye L, Han YW, Bai H et al (2020) *ACS Sustain Chem Eng* 8:7403–7413
- Zhang TW, Li WZ, An SX et al (2018) *Bioresour Technol* 264:261–267
- Bu CY, Yan YX, Zou L (2020) *Bioresour Technol* 313:123705
- Chen LF, Ye JY, Yang YS et al (2020) *ACS Catal* 10:7240–7249
- Fan Y, Li S, Wang Y et al (2020) *Nanoscale* 12:18296–18304
- Merlo AB, Vetere V, Ruggera JF (2009) *Catal Commu* 10:1665–1669
- Vargas-Hernández D, Rubio-Caballero JM, Santamaría-González J et al (2014) *J Mol Catal A Chem* 383–384:106–113
- Cao Y, Noël T (2019) *Org Process Res Dev* 23:403–408
- Deng T, Xu G, Fu Y (2020) *Chin J Catal* 41:404–414
- Belay N, Boopathy R, Voskuilen G (1997) *Appl Environ Microb* 63:2092–2094
- Diaz De Villegas ME, Villa P, Guerra M et al (1992) *Acta Biotechnol* 12:351–354
- Yan YX, Bu CY, Huang X et al (2019) *J Chem Technol Biotechnol* 94:3825–3831
- Yan YX, Bu CY, He Q et al (2018) *RSC Adv* 8:26720–26727
- He YC, Liu F, Di JH et al (2016) *Ind Crop Prod* 81:129–138
- Jiang CX, He YC, Chong GG et al (2017) *J Biotechnol* 259:73–82
- Deng S, Liu X, Liao J et al (2019) *Chem Eng J* 375:122086
- Ferrari AC, Robertson J (2000) *Phys Rev B: Condens Matter Mater Phys* 61:14095–14107
- Ionescu MI, Laforgue A (2020) *Thin Solid Films* 709:138211
- Sosa LF, da Silva VT, de Souza PM (2020). *Catal Today*. <https://doi.org/10.1016/j.cattod.2020.08.022>
- Yadav M, Dasgupta K (2020) *Chem Phys Lett* 748:137391
- Le Guenic S, Delbecq F, Ceballos C et al (2015) *Mol Catal* 410(2015):1–7
- Gómez Millán G, Hellsten S, King AWT et al (2019) *J Ind Eng Chem* 72:354–363
- Gómez Millán G, El Assal Z, Nieminen K et al (2018) *Fuel Process Technol* 182:56–67
- Chen FF, Zhang YH, Zhang ZJ et al (2019) *J Org Chem* 84:14987–14993
- Jin LQ, Yang B, Xu W et al (2019) *Bioresour Technol* 285:121344
- Li QH, Dong Y, Chen FF et al (2018) *Chin J Catal* 39:1625–1632
- Zhang Y, Han B, Ezeji TC (2012) *New Biotechnol* 29:345–351
- Arias PL, Cecilia JA, Gandarias I et al (2020) *Catal Sci Technol* 10:2721–2757
- Li XY, Lu XB, Liang M et al (2020) *Waste Manage* 108:119–126
- Xue XX, Ma CL, Di JH et al (2018) *Bioresour Technol* 268:292–299
- Li X, Liu Q, Si C, Lu L, Luo C, Gu X, Liu W, Lu X (2018) *Ind Crop Prod* 120:343–350
- Feng XQ, Li YY, Ma CL et al (2020) *RSC Adv* 10:40365
- Kijenski J, Winiarek P, Paryjczak T (2002) *Appl Catal A* 23:171–182
- Casoni AI, Hoch PM, Volpe MA et al (2018) *J Clean Prod* 178:237–246
- Hu F, Wang Y, Xu S et al (2019) *Catal Lett* 149:2158–2168
- da Silva MJ, Rodrigues AA (2020) *Mol Catal* 493:111104

Publisher's Note Springer Nature remains neutral with regard to jurisdictional claims in published maps and institutional affiliations.

Authors and Affiliations

Qi Li¹ · Yun Hu¹ · Yong-You Tao¹ · Peng-Qi Zhang¹ · Cui-Luan Ma¹ · Yu-Jie Zhou¹ · Yu-Cai He^{1,2,3}

¹ State Key Laboratory of Biocatalysis and Enzyme Engineering, Hubei Collaborative Innovation Center for Green Transformation of Bio-resources, Hubei Key Laboratory of Industrial Biotechnology, School of Life Sciences, Hubei University, Wuhan, China

² National–Local Joint Engineering Research Center of Biomass Refining and High–Quality Utilization, School of Pharmacy, Changzhou University, Changzhou, China

³ Jiangsu Key Laboratory for Biomass-Based Energy and Enzyme Technology, Huaiyin Normal University, Huaian, China